Journal of Marine Research, 66, 325–345, 2008

On the effect of a sill on dense water formation in a marginal sea

by Doroteaciro Iovino[1,2,3,4], Fiammetta Straneo[5] and Michael A. Spall[5]

ABSTRACT

The properties of water mass transformation in a semi-enclosed basin, separated from the open ocean by a sill and subject to surface cooling, are analyzed both theoretically and numerically using an ocean general circulation model. This study extends previous studies of convection in a marginal sea to the case with a sill.

The sill has a strong impact on both the properties of the dense water formed in the interior and on those of the waters flowing out the marginal sea. It results in a colder interior and colder outflow compared to the case with no sill. Dynamically, this is explained by considering that the sill limits the geostrophic contours over which the open ocean/marginal sea exchange can occur. The impact of the sill, however, is not simply limited to a topographic constriction; instead the sill also decreases the stability of the boundary current, which, in turn, results in relatively large heat flux into the interior and colder outflow.

The theories that relate the properties of the dense waters formed in the interior, and those of the outflow, are modified to include the impact of the sill. These are found to compare well with the numerical simulations and provide a useful tool for the interpretation of these results. These idealized simulations capture the basic features of the water mass transformation processes in the Nordic Seas and, in particular, provide a dynamical explanation for the difference between the dense waters formed and the source of the overflows water.

1. Introduction

Open ocean convection is thought to be an essential ingredient of the present climate system and to play an important role in maintaining the global thermohaline circulation (Marotzke, 2000; Rahmstorf, 2002). Models show that variations in the intensity and location of convection in a few selected regions (the Nordic Seas, the Labrador Sea, and the Weddell Sea) impact the oceanic transports of heat and volume (IPCC, 2007; Rahmstorf, 2002). Given the observed increase in the global temperature, there is a growing need to improve our understanding of deep convection and its variability.

One aspect of convection, which has received much attention over the last few decades,

1. Nansen Environmental and Remote Sensing Center, Thormøhlensgate 47, N-5006 Bergen, Norway.
2. Bjerknes Center for Climate Research, Bergen, Norway.
3. Present address. LOCEAN-CNRS, Université Pierre et Marie Curie, 75252 Paris Cedex 05, France.
4. Corresponding author. ***email: dilod@locean-ipsl.upmc.fr***
5. Woods Hole Oceanographic Institution, Woods Hole, Massachusetts, 02543, U.S.A.

is the actual densification of waters in the interior of convective basins (e.g. Jones and Marshall, 1993; Visbeck *et al.*, 1996; LabSea Group, 1998). The general idea behind these works is that the dense waters are produced in the center of basins, such as the Greenland Sea, the Labrador Sea and the northwestern Mediterranean Sea, which are characterized by a weak stratification and subject to a strong buoyancy loss (Marshall and Schott, 1999). The main goal of these studies was to understand, and hence improve parameterizations of the rapid convective process that occurs in the winter and the dispersal of dense waters from the formation region. What these studies did not address, however, is the connection between the convective region and the surrounding ocean circulation. Ultimately, it is through this exchange that convective regions receive the heat needed to offset the net heat loss to the atmosphere and dense water is removed.

More recently, a number of studies have sought to describe the dense water formation process as one component of a larger setting (Spall, 2003; 2004; Straneo, 2006b). The new paradigm aims to describe not just the open ocean convective region, but also the entire marginal sea/semi-enclosed basin in which convection occurs. In this framework, dense water formation occurs in the interior of a marginal sea that is subject to a net heat loss at the surface. This heat loss is balanced by a cyclonic boundary current that advects warm water into the basin and exports cold water out of it. Heat is supplied from the boundary current to the interior through eddies that result from instabilities of the boundary current. The interior is, on average, a quiescent region where deep and intermediate convection occurs. The boundary current thus plays a fundamental role and its stability has a strong impact on the properties of the dense water formed within the basin. The applicability of this paradigm for the Labrador Sea is supported by the analysis of both historical and modern data (Straneo, 2006a).

One feature common to several convective marginal seas (such as the Nordic Seas or the Mediterranean), which is not included in this new dynamic description, is the presence of a sill. Since a sill affects the exchange between the marginal sea and the open ocean, we expect it to have an impact on the dense water formation that occurs in the marginal sea. Evidence that the sill's characteristics influence dense water formation processes is provided by the model simulations of Roberts and Wood (1997), who analyzed the sensitivity of the large-scale circulation in a coarse-resolution ocean model to slight modifications of topography in the Greenland-Scotland Ridge. They found that these changes have a significant impact on the location of water mass formation, the transport of dense water over the ridge and the poleward heat transport. Similarly, in a more idealized configuration, Walin *et al*. (2004) investigate the role of a sill that connects two bowl-shaped basins, the northernmost one of which is subject to cooling. They find that the sill depth regulates the volume and heat transports between the two basins: a deeper sill results in larger transports. Also, they find that the sill limits the depth of the flow into the 'cold basin' and that this baroclinic flow is transformed into a barotropic slope current while encircling the basin.

Neither of these studies, however, explicitly addresses the dynamical role of the sill in

that class of convective marginal seas that are separated from the major ocean basins by such a topographic feature. In this study, we address this question by extending the theory developed by Spall (2004) and Straneo (2006b) for a convective basin to one that is bound by a sill. In particular, we are interested in determining what influence the sill has on the properties of the dense water produced within the marginal sea, and on the flows into and out of the basin. To do this, we explore the dynamical consequences of the topographic constraint on the marginal sea circulation. We approach this problem with a set of numerical experiments as well as with theoretical arguments. An analysis of the properties of the water formed in the interior of the basin and of the water exported from the basin for varying sill geometry is presented. The basin configuration is idealized to allow for a simple representation of the geometric parameters, and to quantify their influence on the variables of interest. Our study is restricted to basin configurations in which the sill and strait geometries do not result in hydraulically controlled exchange flow over the sill.[6]

The paper is structured as follows. Section 2 presents the primitive equation model used in the numerical sensitivity study. A comparison between numerical simulations with and without a sill is presented in Section 3. The theoretical issues, used to estimate the proprieties of the water masses as function of the sill configuration, are presented and compared to numerical model results in Section 4. A summary and conclusions are presented in Section 5.

2. Numerical model

A set of numerical simulations is carried out with the MIT general circulation model (Marshall *et al.*, 1997a,b) to analyze the thermally driven circulation in an idealized semi-enclosed marginal sea. The model configuration closely follows that used by Spall (2004). The model solves the momentum and density equations on a staggered C-grid in the horizontal and with z coordinates in the vertical. The domain is 1200 km by 1500 km wide and 2200 m deep (Fig. 1). The horizontal grid spacing is 10 km, and there are 16 vertical levels with a resolution ranging from 100 m at the surface to 250 m at the bottom. The model retains a free surface, and uses Cartesian coordinates on an *f*-plane, with the Coriolis parameter $f = 10^{-4}\ \mathrm{s}^{-1}$.

Laplacian parameterizations of viscosity and diffusivity are used. Horizontal and vertical viscosities are 100 $\mathrm{m}^2\ \mathrm{s}^{-1}$ and $5 \times 10^{-4}\ \mathrm{m}^2\ \mathrm{s}^{-1}$, respectively; whereas horizontal and vertical diffusivities are 50 $\mathrm{m}^2\ \mathrm{s}^{-1}$ and $5 \times 10^{-5}\ \mathrm{m}^2\ \mathrm{s}^{-1}$, respectively. No-slip boundary condition is applied, and there are no heat and mass fluxes through the solid boundaries. The time step for the baroclinic component is 1500 s.

The density ρ depends linearly on temperature, so that $\rho = \rho_0 - \alpha(T - T_b)$ where ρ_0 is the reference density for seawater, $\alpha = 0.2\ \mathrm{kg\ m}^{-3}\ ^\circ\mathrm{C}^{-1}$ is the thermal expansion coefficient, and $T_b = 4^\circ\mathrm{C}$ is the initial temperature at the bottom. An annual cycle of sea-surface cooling of

6. The case of hydraulically controlled exchange between an open ocean and a marginal sea with cyclonic boundary currents is considered by Pratt and Spall (2008).

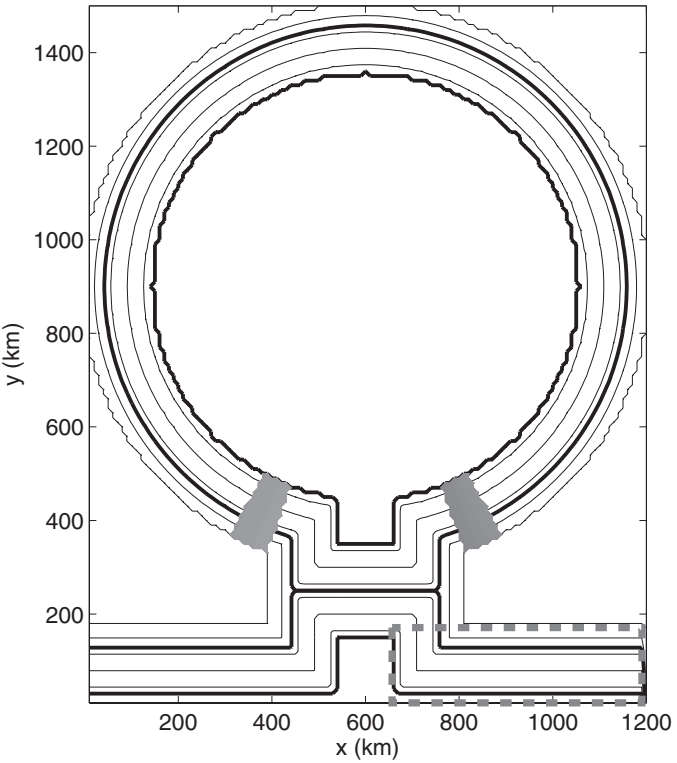

Figure 1. Basin configuration used in the numerical simulation with a sill at 800 m. Contour interval is 500 m. 800 m and 2200 m isobaths are also included (thick black lines). The dashed rectangle indicates the region where the model temperature is restored. Grey areas are used for calculations shown in Figures 4 and 5.

200 W m^{-2} is applied over the marginal sea for 2 months, followed by no forcing for 10 months (the resulting annual mean ocean heat loss is 33 W m^{-2}). Any spatial variability that arises in the solutions is thus a result of lateral advection in the ocean.

Water from the open ocean is supplied to balance the cooling in the marginal sea. This is achieved by restoring the temperature within the dashed rectangle in the open ocean (Fig. 1) toward the linear profile ($T_b + k(z_b - z)$), where z_b is the maximum bottom depth and $k = 1.5 \times 10^{-3}$°C m^{-1} the vertical temperature gradient, with a time scale of 50 days. In this way, the properties of the water flowing into the marginal sea are essentially fixed, independent of what processes take place in the marginal sea. The initial upper-layer temperature is about 7.2°C. The same temperature profile is also used to set the initial uniform stratification. The internal deformation radius—the typical size of eddies in the basin—estimated on the basis of this open ocean stratification is on the order of 20 km, and reasonably well resolved by the horizontal grid spacing.

The circular basin is connected to the ocean through a 400 km wide strait. The

boundaries slope all around the perimeter from 200 m to 2200 m depth over a distance of 140 km, corresponding to a bottom slope of $h_r = 1.43 \times 10^{-2}$. The sill has a meridional extent of 160 km, and is 800 m deep in the reference sill-simulation (Fig. 1). A unique and important aspect of the basin with a sill is the presence of a region of closed geostrophic contours (i.e., closed contours of constant f/H where H is the basin depth, CGC) in the interior, and an outer region of open geostrophic contours (OGC) that connect with the open ocean. A series of experiments are performed that differ only in the strait topography, varying the sill depth from 400 m to 1500 m. This range of sill depths does not result in a hydraulic control of the flow at the strait. The Froude number of our boundary current flowing into the marginal sea is approximately given by the baroclinic deformation radius divided by the width of the boundary current (since the density interface outcrops). The width of the baroclinic boundary current is controlled by the width of the OGC region, which is much wider than the baroclinic deformation radius. Thus, the Froude number is less than 1 for all calculations, and all exchanges are subcritical.

Using this idealized configuration, this study aims at a model formulation that is general and suitable to any marginal sea with similar large-scale characteristics. However, the basin dimensions are chosen to roughly correspond to the Nordic Seas. Similarly, the heat loss from the surface used in this study is close to the average heat flux over the Nordic Seas in the last decades; Blindheim and Østerhus (2005) estimated a yearly mean of net surface heat loss of about 40 W m^{-2} at Jan Mayer for the 1950-2000 period. Obviously this set-up is representative of the Nordic Seas only in a very idealized sense. In particular, the rather complex bathymetry that characterizes the Nordic Seas' interior is neglected. Also, there are no exchanges with the Barents Sea and the Artic Ocean, and only one gateway to the Atlantic Ocean. The basic circulation and governing physics do not appear to be sensitive to variations in the basin dimensions (Spall, 2004). Simulations in a smaller basin of 750 km diameter give results qualitatively similar to the larger basin.

The model has been integrated for 35 years, which allows the simulations to attain essentially a steady state. Most of the results presented below are an average over the last five years.

3. Numerical results

In this section we first describe and compare the qualitative properties of the time-averaged fields of two runs: a basin without sill, essentially reproducing Spall's (2004) simulations, and a basin with an 800 m-deep sill (hereafter referred to as NOSILL and SILL, respectively). In both simulations the circulation over the sloping topography reaches an equilibrium seasonal cycle in less than a decade. The interior takes longer to reach a steady state: in the beginning it cools because the temperature difference between the interior and sloping-bottom regions is not sufficiently large to generate enough eddies from the boundary current to balance the heat loss over the interior. Notably, the interior in NOSILL takes approximately 15 years to reach the steady state compared to more than 20 years in SILL.

a. NOSILL circulation

The general features of the circulation in NOSILL are qualitatively similar to those of Spall (2004). The net heat loss over the marginal sea drives a warm inflow from the open ocean, which travels cyclonically around the basin over the sloping topography (Fig. 2a). The topography around the perimeter of the marginal sea is instrumental in controlling the circulation and the properties of the water masses formed within the basin. The presence of sloping topography sustains the boundary current, which carries warm water into the marginal sea, and, through baroclinic instability, provides eventual restratification of the interior through formation of lateral eddies. Hence, as required to balance the heat budget in the marginal sea, this boundary current cools as it encircles the basin so that the outflow is approximately 0.5°C colder than the inflow, but warmer than the water masses formed in the interior of the marginal sea. The properties of the outflowing water are determined by the exchanges between the cyclonic boundary current and the interior; this interaction is controlled by baroclinic instabilities of the boundary current. The inner flat-bottom region is characterized by the lowest temperatures, approximately 1°C colder than the inflow.

Vertical sections of temperature and velocity show the contrast between the sloping and flat bottom regions (Fig. 3a,b). The water column is warm, strongly stratified and characterized by sharply inclined isopycnals over the sloping boundary. The associated boundary current is surface-intensified with a maximum inflow velocity of about 25 cm s^{-1}. The outflow along the western boundary has a slightly higher maximum velocity and is narrower and deeper than the flow on the eastern side. The velocities in the deep layers increase around the basin, and the net effect is a barotropization of the flow, in agreement with the theory described in Spall (2004), Walin *et al*. (2004), and Straneo (2006b). Over the flat interior, the water column is cold and weakly stratified, with stratification increasing slightly in the upper 100 m. The circulation is cyclonic and much weaker ($\sim$ 5 cm s^{-1}) than over the sloping topography.

In NOSILL, the average depth of the boundary current is approximately one-half the depth of the basin, and its average width equal to the width of the sloping boundary, consistent with simulations presented by Spall (2004). Changes in the bottom slope would result in different boundary current structures: wider sloping boundaries and deeper basins enlarge and deepen the boundary current. Therefore, the topographic configuration of the sloping boundaries partly shapes the boundary current, and therefore influences the baroclinic instability.

b. Changes due to the sill

We find that the presence of the sill at 800 m has a strong impact on the circulation and interior properties of the marginal sea. Both the interior waters and the outflow are about 0.5 °C colder than in NOSILL (Fig. 2b). The portion of the boundary current that changes its temperature around the basin is less wide than in NOSILL and occupies only a fraction (onshore) of the sloping topography. Over the remaining portion, approximately coincid-

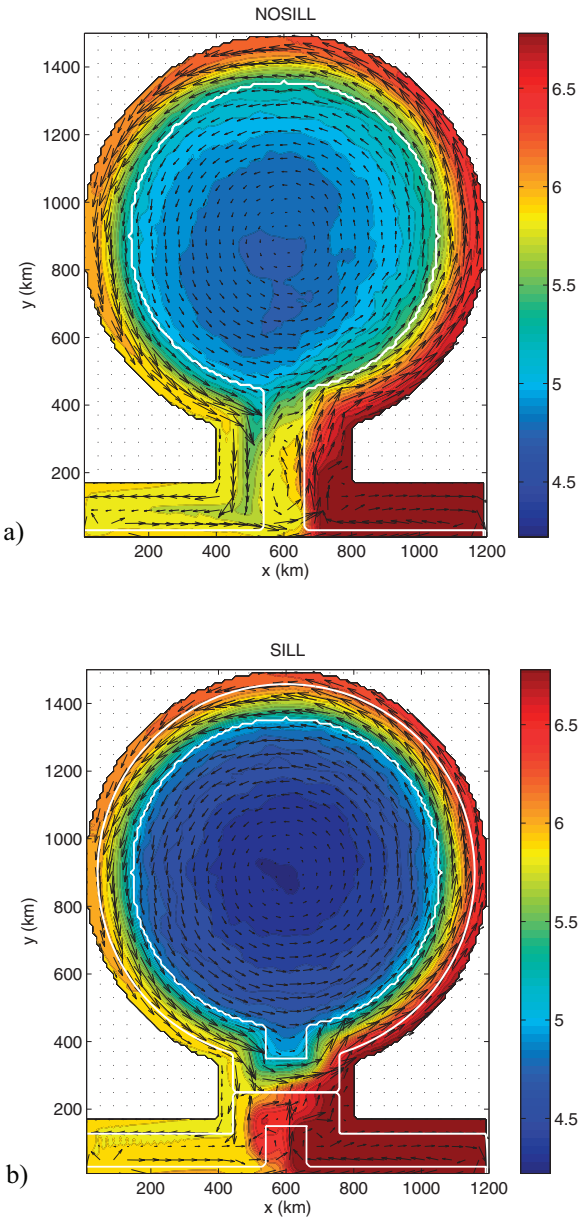

Figure 2. Surface temperature (in °C; contour interval is 0.1°C) and velocity (every fourth grid point), averaged over the last 5 years of model integration for NOSILL (a) and SILL (b). White curves bound the flat bottom interior and also the 800 m contour in the lower panel. The OGC region extends from the coast to the first white isobath.

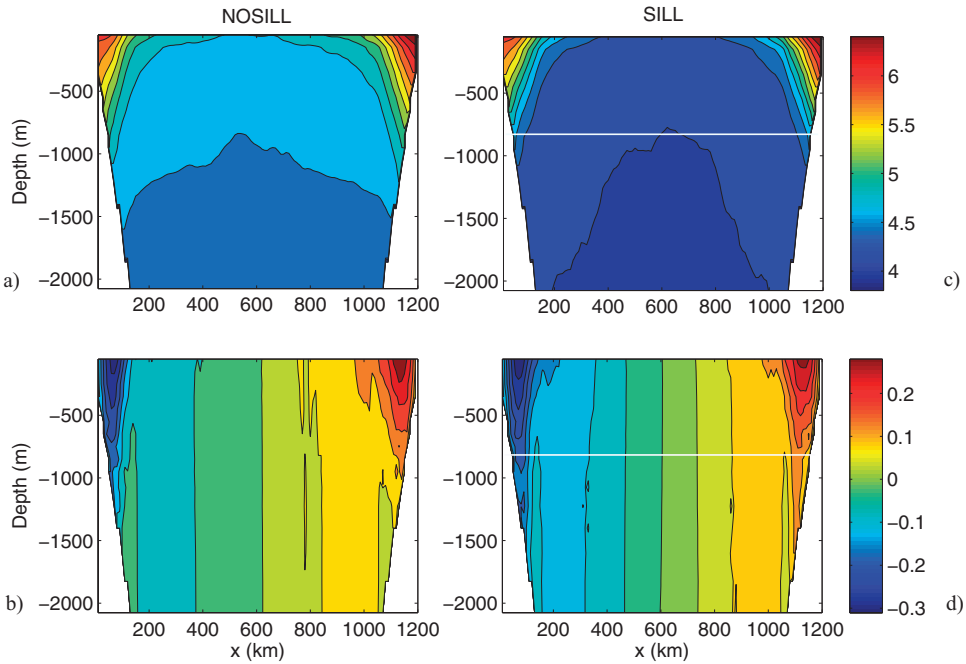

Figure 3. Zonal sections at the mid-latitude of the marginal sea: temperature (in °C; upper panels), and meridional velocity (in m s^{-1}; lower panels) for NOSILL (a, b) and SILL (c, d). Contour interval is 0.2 °C for the temperature, and 0.05 m s^{-1} for the velocity. White lines indicate sill depth.

ing with the closed topographic contours, the boundary current's properties change little around the basin (Fig. 2b).

The sill limits the vertical extent of the warm waters flowing into the basin to sill-depth, as can be seen in the temperature sections shown in Figure 3c. The circulation over the sloping topography is otherwise similar in character to that in NOSILL. The cyclonic circulation in the interior, on the other hand, is stronger than in NOSILL (Fig. 3d).

As described earlier, for the convective marginal sea to be in steady state the boundary current must cool as it flows around the basin. This cooling results both from local air-sea fluxes and from eddy fluxes; their relative magnitude is roughly proportional to the area of the boundary current versus the interior region. Of interest to the problem addressed here is how the cooling of the temperature along the boundary differs once a sill is introduced. We investigate this by comparing the temperature change, across the sloping topography, from inflow to outflow for both cases (Fig. 4). In the case with no sill, the cooling of the boundary current occurs over the entire width of the sloping topography (140 km) and to a depth of approximately 1200 m. With a sill, on the other hand, it is confined to a narrower, onshore portion of the boundary current and to the sill depth (800 m). In both experiments, the width of the portion of the boundary current that loses heat coincides with that of the

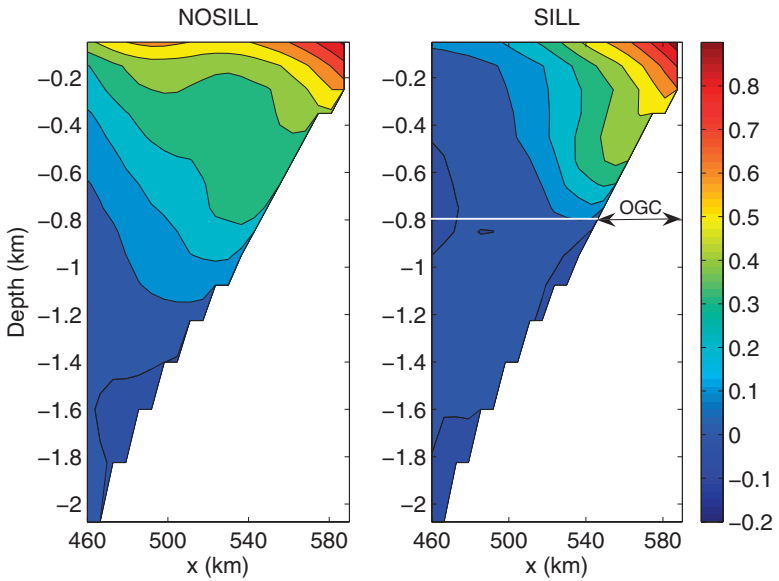

Figure 4. Temperature anomalies of the outflowing water relative to the inflow (in °C, contour interval is 0.1 °C) for NOSILL and SILL. The inflow and outflow temperatures are calculated in the circle sectors indicated in Figure 1, and the difference is projected onto the inflow location. White line indicates the sill depth.

open geostrophic contours (OGC), which, in the presence of a sill, is limited to a fraction of the sloping topography. We note that we do not expect the separation between the two regions to be clear-cut since lateral diffusion acts to smooth the boundary. Nonetheless, it is clear from Figure 4 that the heat loss is concentrated within the OGC region.

The flow of warm water into the marginal sea only occurs over the open geostrophic contours connecting the marginal sea with the large-scale ocean. By limiting the depths over which the two basins are connected, the sill strongly affects the warm inflow. In both experiments, it is the mean advection along these contours that is responsible for supplying the heat, which eddies then transport into the interior that balances the surface cooling. The presence of a sill gives rise to a dynamic region that was absent in NOSILL, a region characterized by sloping topography and closed geostrophic contours (CGC). This region is characterized by a trapped cyclonic recirculation and a negligible mean advection of heat. The surface heat flux is balanced by lateral eddy fluxes, which draw heat from the mean advection along OGC.

c. Sensitivity experiments

A set of experiments has been designed to investigate the sensitivity of water mass properties to variations in the sill configuration. In particular, the experiments differ from SILL only in the depth of the sill, which ranges from 400 m to 1500 m, with increments of 100 m.

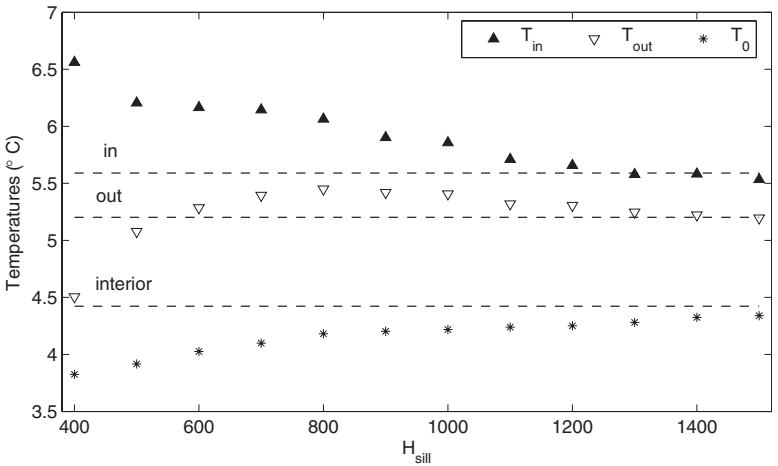

Figure 5. Results of the sensitivity experiments: temperatures (in °C) of the interior, and temperatures (transport weighted) of inflow and outflow as function of sill depth, computed over the OGC in the areas indicated in Figure 1. Dashed lines represent NOSILL temperatures.

We find that the changes in sill depth have an impact on the interior, outflow, and inflowing temperatures (Fig. 5). Inflow and outflow temperatures are here calculated by a transport-weighted integral as $\int_{x_1}^{x_2}\int_{-H}^{0} \mathbf{v}T dxdz / \int_{x_1}^{x_2}\int_{-H}^{0} -\mathbf{v}dxdz$ over the OGC in the sectors indicated in Figure 1. Here **v** is the velocity component perpendicular to the sectors.

The temperature of the interior (T_0, measured at the bottom in the center of the marginal sea) increases, from 3.6 to 4.4°C, as the sill-depth increases. For deep sills, the temperature tends to be that observed in the NOSILL case (Fig. 5)—reflecting the diminishing impact of the sill as this becomes progressively deeper. As shown in Figure 3, the depth of the warm inflow in the NOSILL case is limited to approximately 1200 m; hence, we expect deeper sills to have a small impact on the inflow.

The temperature of the inflow in the sill experiments is larger than that of the NOSILL case because it is weighted over the OGC, and hence confined to the warmer waters trapped over the shallowest part of the topography (Fig. 5). We note, however, that this does not mean that the heat transport into the basin in the SILL experiments is greater than in the NOSILL. The temperature of the outflowing waters, on the other hand, does not exhibit a monotonic behavior but instead is maximum for moderate sill depths. The temperature difference between the inflow and the outflow increases monotonically as the sill depth decreases. In other words, shallower sills are associated with a more substantial cooling of the boundary current than deeper sills. At any rate, we note that $T_{in} > T_{out} > T_0$ for all experiments.

4. Theoretical arguments

Both Spall (2004) and Straneo (2006b) propose idealized, theoretical, dynamic models that relate the characteristics of the dense water formed in a convective basin to the inflow

conditions, the surface heat loss and the geometric parameters of the basin. Within these models, the exchange between the interior and the boundary current is accounted for by relying on parameterizations for the baroclinic instability of the current. In Spall (2004), the theory is developed for the steady state balance within the marginal sea and formulated in terms of temperature and velocity. Straneo (2006b) proposes a similar, but time-varying model, formulated in terms of thickness (for constant density layers) and velocity. In both cases, there are no closed topographic (or geostrophic) contours within the basin so that the exchange with the open ocean (beyond the marginal sea) occurs throughout the boundary current's width. Here, we extend these theoretical models (and that of Spall in particular) to the case of a marginal sea bound by a sill. Our objectives are to gain better insight into the processes responsible for the changes shown in the previous session and to develop a means of quantitatively assessing the impact of the sill.

a. Review of Spall's model

In Spall's (2004) model, the marginal sea is described in terms of three water masses: the waters formed within the interior of the marginal sea, characterized by temperature T_0; the waters flowing into the basin from the open ocean, characterized by temperature T_{in}, thickness H_{in} (where $H_{in} = dH_{tot}$, and d is a constant of $O(1)$, empirically set to 0.65 here), and velocity V_{in}; and the waters flowing out of the basin, temperature T_{out}, thickness H_{out}, and velocity V_{out}. The total depth of the basin is H_{tot}.

The theory is developed by imposing a number of constraints:

1. The net mass transport into the marginal sea is zero: $V_{in}H_{in}L = V_{out}H_{out}L$, where L is the width of the boundary current, taken to be the width of the sloping bottom.

2. The surface heat loss over the marginal sea must be balanced by the advection of heat into and out of the basin: $(\pi R^2 Q/\rho_0 C_p) = T_{in}V_{in}H_{in}L - T_{out}V_{out}H_{out}L$, where R is the radius of the basin, Q the mean surface heat loss (positive upward), ρ_0 the reference density of seawater, and C_p the specific heat capacity of seawater.

3. The flow is in geostrophic balance, such that the inflow is $V_{in} = (\alpha g(T_{in} - T_0)\, H_{in}/L\rho_0 f_0)$ where α is the thermal expansion coefficient, g the gravitational acceleration, and f_0 the Coriolis parameter.

4. In the interior region, which is assumed to have no mean flow, the annual cooling is balanced by the lateral eddy heat fluxes originating from the boundary current at the edge of the flat bottom: $2\pi R_0 H_{in}\overline{u'T'} = (SQ/\rho_0 C_p)$, where R_0 and S are the radius and area of the interior, respectively. The radii of the basin and its interior are not assumed equal, unlike Spall (2004), because of the larger dimensions of the basin.

5. The lateral eddy heat fluxes are parameterized as $\overline{u'T'} = cV_{in}(T_{in} - T_0)$, where c is a nondimensional correlation coefficient, linearly related to the eddy efficiency (Spall, 2004). Its value has been estimated empirically and theoretically to be $O(10^{-2})$ for flat bottom basin (Visbeck *et al.*, 1996; Spall and Chapman, 1998), and

$O(10^{-3})$ for sloping bottom, where it depends on the bottom slope parameter δ, defined as the ratio of the topographic and isothermal slopes, so that $c = 0.025e^{(2\delta)}$ (Spall, 2004). δ is thus fundamental in quantifying the exchange between the warm boundary current and the interior; for a boundary current flowing cyclonically around the basin in absence of sill δ = O(-1) (Spall, 2004).

Making use of these assumptions and constraints, Spall (2004) is able to relate the properties of the dense water formed, the inflow, and outflow to the basic geometric parameters of the system and the surface heat loss imposed. In particular, the density of the water formed in the flat-bottom portion of the basin (T_0) relative to the open-ocean temperature (T_{in}), is given by:

$$T_{in} - T_0 = \left(\frac{Sf_0Q}{\alpha g C_p}\right)^{1/2} H_{in}^{-1}\varepsilon^{-1/2} \tag{1}$$

and thus, the inflow velocity becomes

$$V_{in} = \frac{1}{L\rho_0}\left(\frac{\alpha g S Q}{f_0 C_p \varepsilon}\right)^{1/2}. \tag{2}$$

The parameter ε is a nondimensional measure of the eddy efficiency, defined in Spall (2004) as $\varepsilon = 2\pi Rc/L$. In NOSILL, where isotherms intersect the bottom at about the midpoint of the slope and surface on the offshore side of the sloping topography, ε = O (0.1).

The heat balance in the marginal sea requires the outflowing water to be colder than the inflowing water and, in general, warmer than the coldest water formed in the interior of the basin. The temperature decrease between outflow and inflow can be estimated from the balances of heat and mass as function of the fraction of heat fluxed from inflow into the interior by eddies (as derived in Spall, 2004):

$$T_{in} - T_{out} = (T_{in} - T_0)\varepsilon. \tag{3}$$

b. Modified theory for a basin with a sill

The numerical experiments have shown that the introduction of the sill quantitatively impacts the circulation and the properties of the dense water formed, but not the overall processes governing convection in the marginal sea. Thus, we expect the same theoretical arguments developed by Spall (2004) to hold provided one takes into account the modifications introduced by the sill. Physically, we expect the sill to impact convection in two ways: first by limiting the exchange with the open ocean (waters below sill depth are isolated within the marginal sea) and second by modifying the structure of the boundary current and, hence, the eddy exchange. In terms of the theoretical model's parameters, the sill modifies both the thickness of the boundary current and its width.

We assume here that the boundary current is as deep as the sill, $H_{in} = H_{sill}$, and as wide as the portion of sloping boundary above sill depth, i.e. the OGC ($L_{sill} = LH_{sill}/H_{tot}$). Also,

we assume that the change in the isopycnal slope around the basin is negligible and, therefore, that c is constant. These assumptions are supported by the numerical results presented above. As a result of the change in thickness and width of the boundary current, the eddy efficiency in the basin with a sill differs from that without a sill:

$$\varepsilon_{sill} = 2\pi Rc/L_{sill} = \varepsilon_{ref} H_{tot}/H_{sill}. \tag{4}$$

The subscript "ref" indicates a reference case without sill. From the expression above, a shallow sill is characterized by a larger efficiency coefficient than a deeper sill or than a case with no sill. As a result, the boundary current is more unstable because of reduced L_{sill}: for a given ΔT, the horizontal gradients $\delta T/\delta x$ increases and, through thermal wind, so does the vertical gradient $\delta u/\delta z$, which the growth rate for baroclinic instability is proportional to. Thus, a shallow sill results in an increased instability of boundary current.

Similarly, a shallower sill is associated with an increase in the velocity of the inflowing waters with respect to deeper sill or to the no sill case:

$$V_{sill} = \frac{1}{L_{sill}\rho_0}\left(\frac{\alpha g S Q}{f_0 C_p \varepsilon_{sill}}\right)^{1/2} = V_{ref}\left(\frac{H_{tot}}{H_{sill}}\right)^{1/2}. \tag{5}$$

Notwithstanding the increasing velocity, the transport in the boundary current, given by

$$V_{sill} H_{sill} L_{sill} = V_{ref} H_{tot} L (H_{sill}/H_{tot})^{3/2}, \tag{6}$$

decreases because of the reduced depth and width of the flow.

From (1) and (3), replacing the NOSILL parameters with ε_{sill} and H_{sill}, the temperature anomalies of the interior and outflowing waters, relative to the inflow temperature, $T_{in} - T_0$ and $T_{in} - T_{out}$ are given by

$$T_{in} - T_0 = \left(\frac{S f_0 Q}{\alpha g C_p}\right)^{1/2} \frac{1}{H_{sill}\varepsilon_{sill}^{1/2}} = (T_{in} - T_0)_{ref}\left(\frac{H_{tot}}{H_{sill}}\right)^{1/2} \tag{7}$$

and

$$T_{in} - T_{out} = (T_{in} - T_0)_{sill}\varepsilon_{sill} = (T_{in} - T_{out})_{ref}\left(\frac{H_{tot}}{H_{sill}}\right)^{3/2}. \tag{8}$$

The temperature anomaly of the outflowing water, relative to the temperature of the cold waters formed in the interior of the basin, is obtained as

$$T_{out} - T_0 = (T_{in} - T_0)_{sill}(1 - \varepsilon_{sill}) = (T_{in} - T_0)_{ref}\left(\frac{H_{tot}}{H_{sill}}\right)^{1/2}\left(1 - \varepsilon_{ref}\frac{H_{tot}}{H_{sill}}\right). \tag{9}$$

The above expressions illustrate how we expect a basin with a sill to be associated with a colder convected water mass in the interior and colder waters flowing out, with respect to a basin with no sill. If the inflow water temperature were the same, temperature contrast between the interior and inflow waters and, also, between the inflow and outflow waters are

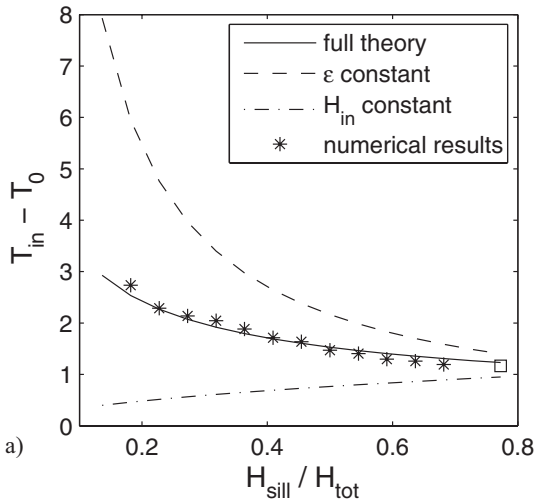
full theory
ε constant
H_in constant
numerical results
T_in – T_0
H_sill / H_tot
a)

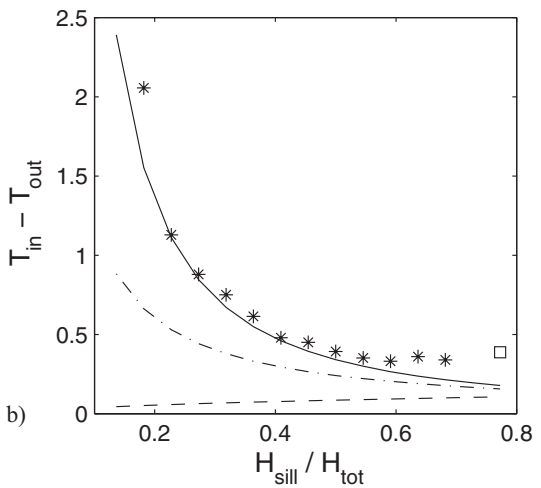
T_in – T_out
H_sill / H_tot
b)

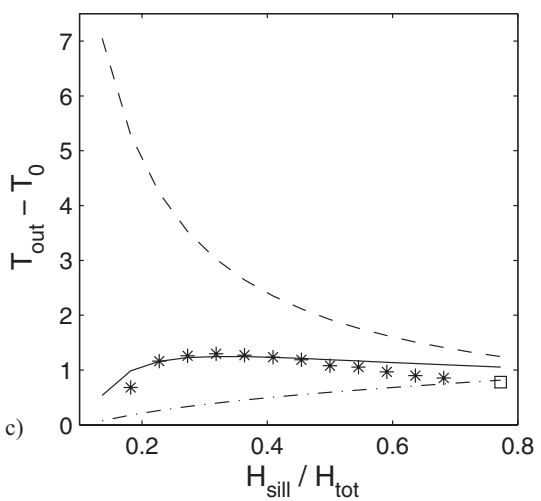
T_out – T_0
H_sill / H_tot
c)

larger. Note also the different dependence of the two temperature anomalies on the sill depth. The inflow/outflow temperature difference contrast is more sensitive to the sill depth than the interior/inflow contrast. The difference between the outflowing waters and the interior waters is not immediately evident and depends on the value of ε and H_{sill}. For small ε or deep sills, $T_{out} - T_0$ increases with decreasing sill depth, while for large ε or shallow sills, $T_{out} - T_0$ decreases with decreasing sill depth. That suggests the presence of two competing effects of the sill, as discussed in the following section.

c. Comparison with numerical model

Expressions (7) and (8) are compared to the interior and outflow temperature contrast in the numerical experiments with varying sill depth, Figure 6. Overall, we find good agreement between the theory and the numerical solutions, with a correlation of 0.99 (0.97) and a least square line of slope 1.22 (1.19) for T_0 (T_{out}). It is worth pointing out that both theory and numerical solutions show that the outflowing water is always warmer than the interior water (Fig. 6c), but that there exists a sill depth for which the difference is maximum. The maximum occurs for $H_{sill} = 3\varepsilon H_{tot}$ or about 700 m for $H_{tot} = 2200$ m.

As mentioned earlier, the sill affects the convective process in two ways: by limiting the exchange with the open ocean and by affecting the stability of the boundary current. The theory allows us to investigate their impact separately. First, we consider the effect of blocking (limited exchange) alone by neglecting the change in ε (using the NOSILL value of $2\pi Rc/L$) but allowing changes in the flow thickness (H_{in}) alone in (7) and (8). Both expressions predict that, in this case, the temperature differences are inversely proportional to the sill depth, as shown in Figure 6 (curves labeled ε constant). Compared to the full theory and to the numerical solutions, this analysis shows that though the tendency for the interior temperature is correct (colder interior for shallower sills), by not including variations in the eddies' efficiency the interior is too cold and the outflow is too warm.

Next, we consider the impact of the change in the eddy efficiency alone on T_0 and T_{out} by keeping H_{in} constant while allowing ε to depend on the sill depth. The change in the boundary current stability, due to the sill, tends to produce a warmer interior and a colder outflow since the increasingly unstable boundary current is able to release more heat to the interior. This tendency is opposite to that due to the blocking (Fig. 6; curves labeled H_{in} constant).

We calculate the volume transport in the inflow boundary current when it crosses the sill between the coast and the isobath H_{sill}, for each numerical case. Deeper sills result in larger volume exchanges between the open ocean and the marginal sea (Fig. 7), corroborating the primary importance of the sill for the exchanges in the present simulations. We

←

Figure 6. Comparison between (a) the temperature anomalies (in °C) of the interior (T_0) and (b) outflowing waters (T_{out}) relative to the inflow temperature (T_{in}) computed from the set of numerical simulations (stars) and from the theoretical calculations as function of H_{in} and ε. (c) Comparison for the anomaly $T_{out} - T_0$ (in °C). Squares indicate numerical NOSILL calculations.

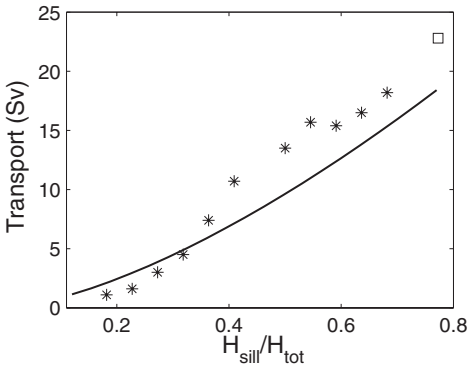

Figure 7. Comparison between the volume transport (in Sv) in the inflow boundary current at the sill computed for the set of numerical simulations (stars) and from the theoretical calculations as function of H_{in}. Square indicates numerical NOSILL calculation.

compare the simulated transports with the estimates (6). Numerical results slightly overestimate the theoretical predictions for deep sills, but the comparison (shown in Fig. 7 as function of the sill depths) presents a good qualitative agreement.

This analysis indicates that, while the greatest impact of the sill is to limit the exchange with the open ocean, and hence allow less warm water to flow into the basin, the interior is not as cold as one might expect. This is because the sill also impacts the boundary current's stability allowing relatively more heat to be fluxed by eddies into the interior. The boundary current is more unstable because the dynamically active part of the boundary current is confined to the OGC, so that the lateral density gradient and the vertical shear in the velocity are increased. Hence, the warmer convective product and the colder than expected outflow.

d. Change around the basin

In the dynamics described above, the cooling in the interior of the marginal sea is balanced by the release of heat from the boundary current. As a result, the boundary current cools as it flows around the basin. How rapidly the boundary current cools can be predicted from the theory of Straneo (2006b). Let $T(l) = T_{in} + T_d(l)$, where T_d is the temperature decay along the perimeter and (l) is the coordinate around the perimeter of the basin. Under the assumption that the amount of heat exchanged by eddies is smaller than the heat transported around the basin, $T_d \ll T_{in} - T_0$, we can re-write Straneo's (2006b) expression for the rate of change in terms of the change in temperature around the basin:

$$T_d(l) = (T_{in} - T_0)(1 - e^{-2l\varepsilon/P}) \tag{10}$$

where P is the perimeter of the basin. Thus the theory predicts that the temperature will decay exponentially around the basin and that the decay will tend to zero as the boundary current/interior temperature difference tends to zero.

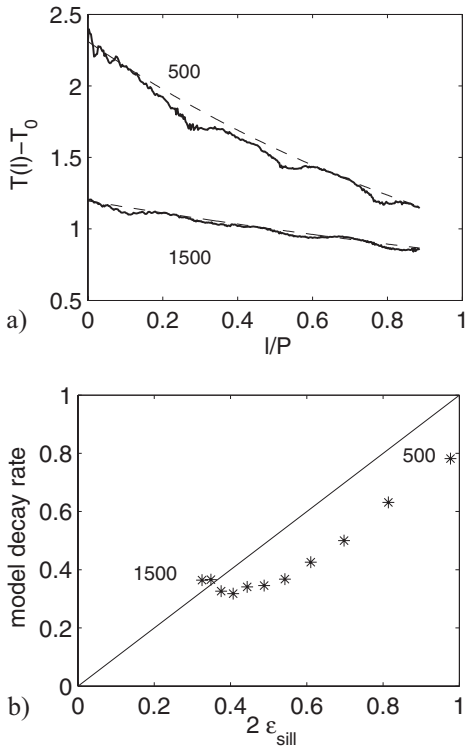

Figure 8. (a) Decay of the interior/boundary current temperature difference $T(l) - T_0$ (in °C, with $T(l)$ integrated over the OGC) as a function of the normalized perimeter (solid lines) for the model simulations with a sill at 1500 m and 500 m. Overlaid on each curve is a least square exponential fit (dashed lines). (b) Model decay rate (squares, see text for definition) plotted as function of $2\varepsilon_{sill}$. The straight line represents the decay rate predicted by the theory.

In the case of a basin with a sill, the eddy efficiency parameter (ε_{sill}) that modulates the decay rate is inversely proportional to sill depth. Physically, this implies that the eddies are relatively more efficient at extracting the heat in a basin with a shallow sill than in a basin with a deep sill. The qualitative agreement between the theory and the numerical results is shown in Figure 8a where we compare the temperature change in the boundary current (relative to the interior temperature) around the basin's perimeter for a shallow sill and a deep sill experiment. Overlaid on the two curves is the respective exponential least square fit. As predicted by the theory the temperature in the experiment with a sill at 500 m decreases much faster than that with a sill at 1500 m.

A more quantitative comparison of the decay rate in the numerical simulations versus that predicted by the theory is shown in Figure 8b. For each experiment we calculate the decay rate of the boundary current temperature around the perimeter (relative to the interior temperature) by least square fitting an exponential curve (as shown for two cases in

Fig. 8a). The decay rate of this exponential fit, normalized by l/P, is then compared to that predicted by the theory, $2\varepsilon_{sill}$, from the equation above. Overall, we find good agreement between the linear decrease in the decay rate as the sill depth increases predicted by the theory and found in the numerical experiments. We note that one expects a departure from the theoretically predicted decay rate since the theory assumes that the eddy fluxes do not substantially modify the structure of the boundary current (Straneo, 2006b). For shallower sills, the increase in eddy efficiency implies a more substantial modification of the current structure around the basin, which, in turn, means we are no longer in the linear regime assumed in Eq. (10). Finally, since the impact of the sill is negligible for sills deeper than $H_{in}/2$, we do not expect the decay rate to vary as a function of sill parameters for these deeper sills.

5. Summary and conclusions

We have investigated the impact of a sill on convection in a semi-enclosed basin using both an eddy-resolving numerical model and theory. Previous studies on convection in a semi-enclosed basin, subject to cooling, showed that the net heat loss to the atmosphere is balanced by lateral advection from the open ocean via a warm boundary current that moves cyclonically around the basin. The gradient between the warm boundary current and the cold interior gives rise to instability of the current, which, in turn, results in the advection of heat into the interior by mesoscale eddies. The properties of the dense waters formed in the interior and of the dense water exported out of the basin have been shown to be a function of the topographic parameters of the basin, of the surface cooling and of the efficiency with which the eddies can flux heat into the interior.

We found that the sill plays an important role in setting the properties of the dense waters formed inside the basin and of the outflow. Explicitly, a basin with a sill results in a colder convective product and in a colder outflow compared to the case with no sill, all other parameters being equal. This can be explained by considering that the sill limits the thickness and width of the inflowing warm boundary current. Dynamically, it restricts the geostrophic contours that connect the marginal sea to the open ocean (the open geostrophic contours) and results in a region of closed geostrophic contours in the interior of the basin. While the boundary current, in the marginal sea, is distributed across the entire sloping topography, our numerical simulations show that the mean advection of heat into the basin, and the release of heat to the interior occur only along the open contours. The closed geostrophic contours in the basin's interior are associated with a mean recirculating flow but no significant change in heat content. The shallower the sill the more these effects are enhanced.

The theories developed for basins with no sill have been modified to include the effect of the sill and compare well with the numerical experiments conducted. The theoretical analysis shows that the introduction of a sill affects the convective process via two competing mechanisms. On one hand it limits the exchange with the open ocean and hence the advection of heat into the basin (the blocking effect). On the other hand, it increases the

instability of the boundary current flowing into the basin, primarily by modifying its width, and hence the eddy flux of heat into the interior. As a result, the interior is not as cold as one would expect given the blocking effect of the sill. On the other hand, the outflow is notably colder than in the absence of a sill.

In terms of the effect on the boundary current, we find that for basins with a shallow sill the boundary current tends to cool much more than for basin with a deep sill. This reflects the increasing impact of the eddy fluxes on the current itself. This behavior is predicted by the theory once the impact of the sill on the eddy efficiency is taken into account.

We believe that our idealized system captures the dominant features of the water mass transformation process in semi-enclosed basins separated by a sill. Using the Nordic Seas as an example, the circulation in the model is consistent with the inflow of warm Atlantic waters over the Greenland-Scotland Ridge and their progressive transformation (cooling and densification) as they flow cyclonically along the topographic boundaries and around the dense waters formed in the Iceland, Norwegian and Greenland seas. Similar to the model simulations, the Atlantic water's thickness is comparable to sill depth (Blindheim and Østerhus, 2005). Given this analogy, our study provides us with a dynamical context that supports the distinction between the dense waters formed in the interior of the basin and those exported into the open ocean. In the case of a basin with a sill, the dense waters are confined to the marginal sea whereas the outflow waters are the transformed inflow waters. As shown by our theoretical analysis, and supported by the numerical experiments, the sill results in a decrease in the temperature difference between the outflowing waters and the interior convective product. This supports, in part, the description of Mauritzen (1996a,b) who argues that the waters flowing out the Nordic Seas have been made dense along their mean advective path and do not come from the dense water formation regions of the Nordic Seas. At the same time, our study shows that the lateral eddy exchange with the interior plays an important role in modifying the inflow, while Mauritzen's studies attribute much of the transformation to the surface fluxes alone. The distinction between the outflow waters and the dense interior product is an important one since the outflow waters are, in the case of the Nordic Seas, the source waters for the overflows to the North Atlantic and of relevance to the overturning circulation. This perspective disagrees with a traditional point of view that considers the overflows to be the result of deep convection in the internal gyres of the Nordic Seas (e.g., Aagaard *et al.*, 1985; Hopkins, 1991). A second important result of our study is that the sill tends to increase the instability of the inflowing warm waters. Effectively this means increased eddy fluxes and rapid removal and dispersal of heat from the inflow. This is qualitatively consistent with the rapid spreading and cooling of the Atlantic warm waters as they enter the Nordic Seas and may help explain the active eddy field which spreads the Atlantic water across the Lofoten Basin (Jakobsen *et al.*, 2003).

This study is idealized in nature and neglects a number of important features of the circulation of the Nordic Seas. There is no freshwater component in our model, which likely plays a thermodynamic role in setting the properties of the dense water formed

(Broström and Ferrow, 2008). Also, the topography of the basin is highly idealized, compared to the real Nordic Seas, and there is no wind forcing, which undoubtedly plays a role in the variability of the exchange between the North Atlantic and the Nordic Seas (Furevik and Nilsen, 2005). Nonetheless, by focusing on this simpler system, we feel that we have been able to isolate the primary effect of a sill on the buoyancy-forced circulation within a marginal sea and its exchange with the open ocean.

Acknowledgment. DI was supported by the Polar Ocean Climate Processes (ProClim) project funded by the Norwegian Research Council. FS was supported by a visiting scientist fellowship from the Bjerknes Centre for Climate Research (Bergen, Norway) and by NSF Ocean Sciences Grant 0525929. Support for MAS was provided by NSF Office of Polar Programs Grant 0421904 and NSF Ocean Sciences Grant 0423975.

REFERENCES

Aagard, K., J. H. Swift and E. C. Carmack. 1985. Thermohaline circulation in the Arctic Mediterranean seas. J. Geophys. Res., *90*, 4833–4846.

Blindheim, J. and S. Østerhus. 2005. The Nordic Seas, Main Oceanographic Features, *in* The Nordic Seas: An Integrated Perspective, H. Drange, T. M. Dokken, T. Furevik, R. Gerdes, and W. Berger, eds., Amer. Geophys. Union, Washington DC, USA, 11–38, AGU Monograph 158.

Broström, G. and A. Ferrow. 2008. Dual buoyancy forcing in semi–enclosed seas: An idealized study of the Arctic Mediterranean. J. Mar. Res. (submitted).

Furevik, T. and J. E. Ø. Nilsen. 2005. Large–scale atmospheric circulation variability and its impacts on the Nordic Seas ocean climate—a review, *in* The Nordic Seas: An Integrated Perspective, H. Drange, T. M. Dokken, T. Furevik, R. Gerdes and W. Berger, eds., American Geophysical Union, Washington DC, USA, AGU Monograph 158, 105–136.

Hopkins, T. S. 1991. The GIN Sea—a synthesis of its physical oceanography and literature review 1972–1985. Earth Sci. Rev., *30*, 175–318.

IPCC. 2007. Climate Change 2007: The Physical Science Basis. Working Group I Contribution to the Forth Assessment Report of the Intergovernmental Panel on Climate Change. Cambridge University Press, Cambridge.

Jakobsen, P., M. Ribergaard, D. Quadfasel, T. Schmith and C. Hughes. 2003. Near–surface circulation in the northern North Atlantic as inferred from Lagrangian drifters: Variability from the mesoscale to interannual. J. Geophys. Res., *108(C8)*, 3251, doi:10.1029/2002JC001554.

Jones, H. and J. Marshall. 1993. Convection with rotation in a neutral ocean. A study of open–ocean deep convection. J. Phys. Oceanogr., *23*, 1009–1039.

LabSea Group. 1998. The Labrador Sea Deep Convection Experiment. Bull. Amer. Meteor. Soc., *79*, 2033–2058.

Marotzke, J. 2000. Abrupt climate change and thermohaline circulation: Mechanisms and predictability. Proc. Nat. Acad. Sci. (U.S.A.), *97*, 1347–1350.

Marshall, J., A. Adcroft, C. Hill, L. Perelman and C. Heisey. 1997a. A finite–volume, incompressible Navier Stokes model for studies of the ocean on parallel computers. J. Geophys. Res., *102(C3)*, 5753–5766.

Marshall, J., C. Hill, L. Perelman and A. Adcroft. 1997b. Hydrostatic, quasi–hydrostatic, and nonhydrostatic ocean modeling. J. Geophys. Res., *102(C3)*, 5733–5752.

Marshall, J. and F. Schott. 1999. Open ocean deep convection: observations, theory and models. Rev. Geophys., *37*, 1–64.

Mauritzen, C. 1996a. Production of dense overflow waters feeding the North Atlantic across the

Greenland–Scotland Ridge. Part 1: Evidence for a revised circulation scheme. Deep–Sea Res. I, *43*, 769–806.

—— 1996b. Production of dense overflow waters feeding the North Atlantic across the Greenland–Scotland Ridge. Part 2: An inverse model. Deep–Sea Res. I, *43*, 807–835.

Rahmstorf, S. 2002. Ocean circulation and climate during the past 120,000 years. Nature, *419*, 207–214.

Pratt, L. J. and M. A. Spall. 2008. Circulation and exchange in choked marginal seas. J. Phys. Oceanogr. (in press).

Roberts, M. J. and R. A. Wood. 1997. Topographic sensitivity studies with a Bryan–Cox–Type ocean model. J. Phys. Oceanogr., *27*, 823–836.

Spall, M. A. 2003. On the thermohaline circulation in flat bottom marginal seas. J. Mar. Res., *61*, 1–25.

—— 2004. Boundary currents and water mass transformation in marginal seas. J. Phys. Oceanogr., *34*, 1197–1213.

—— 2005. Buoyancy–forced circulations in shallow marginal seas. J. Mar. Res., *63*, 729–752.

Spall, M. A. and D. C. Chapman. 1998. On efficiency of baroclinic eddy heat transport across narrow fronts. J. Phys. Oceanogr., *28*, 2275–2287.

Straneo, F. 2006a. Heat and freshwater transport through the central Labrador Sea. J. Phys. Oceanogr., *36*, 606–628.

—— 2006b. On the connection between dense water formation, overturning, and poleward heat transport in a convective basin. J. Phys. Oceanogr., *36*, 1822–1840.

Visbeck, M., J. Marshall and H. Jones. 1996. Dynamics of isolated convective regions in the ocean. J. Phys. Oceanogr., *26*, 1721–1734.

Walin G., G. Broström, J. Nilsson and O. Dahl. 2004. Baroclinic boundary currents with downstream decreasing buoyancy; A study of an idealized Nordic Seas system. J. Mar. Res., *62*, 517–543.

Received: *8 October, 2007*; revised: *4 June, 2008*.